Coordination-supported Organic Polymers: Mesoporous Inorganic-Organic Materials with Preferred Stability

Journal:	*Inorganic Chemistry Frontiers*
Manuscript ID	QI-RES-05-2018-000471
Article Type:	Research Article
Date Submitted by the Author:	22-May-2018
Complete List of Authors:	Chen, Dong; Shanghai Jiao Tong University Zhang, Pengfei; Shanghai Jiao Tong University, Department of Chemical Engineering; Oak Ridge National Laboratory, Fang, Qianrong; Jilin University, Department of Chemistry Wan, Shun; Oak Ridge National Lab, Li, Hui; Jilin University Yang, Shize; Oak Ridge National Laboratory, Materials Science Technology Division Huang, Caili; Oak Ridge National Laboratory, ; University of Massachusetts Amherst, Dai, Sheng; Oak Ridge National Laboratory,

Journal Name

COMMUNICATION

Coordination-supported Organic Polymers: Mesoporous Inorganic-Organic Materials with Preferred Stability

Received 00th January 20xx,
Accepted 00th January 20xx

DOI: 10.1039/x0xx00000x

www.rsc.org/

Dong Chen,[a] Pengfei Zhang,[*ab] Qianrong Fang,[c] Shun Wan,[b] Hui Li,[c] Shize Yang,[b] Caili Huang,[b] Sheng Dai,[*bd]

Abstract: A simple and versatile strategy, borrowing ideas from the chemistry of MOFs and COFs, is developed for the synthesis of coordination-supported organic polymers (COPs) via coordination between Al^{3+} and 5-amino-8-hydroxyquinoline together with organic imine- or imide-based polycondensation. The COPs with high surface areas (up to 1123 m^2g^{-1}) and abundant mesopores (2.5 nm or 14 nm) possess good crystalline and porous structure after soaked in boiling water.

Compared to porous inorganic solids (e.g., zeolites and aluminosilicates) that have been well studied and already used in real applications, porous materials—made by organic or inorganic-organic building units are entering what can be described as a “golden” age, when lots of novel materials are emerging with abundant porosity, tunable surface chemistry, specific electronic structure, controlled functional groups and so on.[1-8] Those attractive characters endow them with promising performance in catalysis, separation, gas storage, *etc*.[9-13] Based on the manner of assembly, two classes of organic building blocks are frequently employed (**Figure 1**). Type I refers to organic ligands with two or more coordinating sites that can be joined by metal coordination polymerization,[14-18] while organic linkers with multi reactive groups for covalent bond formation are considered as Type II.[19-25] Certainly, both building blocks should possess some rigidity, which can generate a backbone that is strong enough to stand the intermolecular packing force.

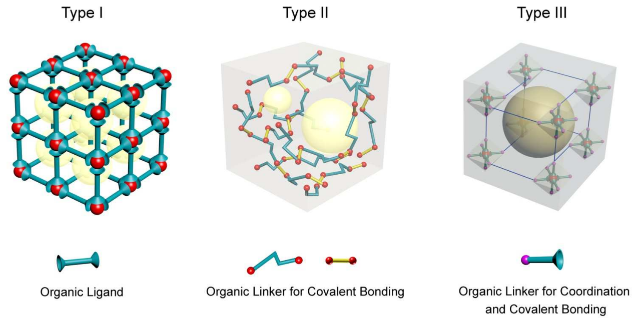

Figure 1. Three classes of building blocks proposed for the design of porous organic materials. Type I: Organic Ligand for metal-organic framework. Type II: Organic Linker for porous polymer via covalent bonding formation Type III: Hybrid building block with both coordination point and covalent linkable group.

As a typical material by **Type I**, highly porous metal-organic frameworks (MOFs) have already shown high uptakes in gas storage and separation.[26-39] However, the poor water stability of many MOFs hinders their way toward practical applications like CO_2 capture, because water vapor from industrial flue gas can make the coordination framework collapse by competing hydrolysis of metal ions.[40-42] In this regard, porous materials with only covalent bonded architecture (**Type II**) such as covalent organic frameworks (COFs), polymers of intrinsic microporosity (PIM), conjugated microporous polymers (CMPs), hyper-cross-linked polymers (HCPs), porous polymer networks, are more tolerable to water and moisture.[43-49] In addition, the porosities of MOFs/COFs are primarily dominated by micropores, whereas mesoporous MOFs/COFs are designed with difficulties due to the stronger packing force, the unsatisfied rigidity of organic backbones and the lack of large building blocks. Such water-resistant microporous MOFs have already been well studied in literature, however, the development of mesoporous water-stable MOFs is still challenging.[50-51]

---

[a] *School of Chemistry and Chemical Engineering, Shanghai Jiao Tong University, Shanghai 200240, China, E-mail: chemistryzpf@sjtu.edu.cn*
[b] *Chemical Sciences Division, Oak Ridge National Laboratory, Oak Ridge, Tennessee 37831, United States, E-mail: dais@ornl.gov*
[c] *State Key Laboratory of Inorganic Synthesis and Preparative Chemistry, Jilin University, Changchun 130012, China*
[d] *Department of Chemistry, University of Tennessee, Knoxville, Tennessee 37996, United States*

†Electronic Supplementary Information (ESI) available: Experimental section and supplementary figures. See DOI: 10.1039/x0xx00000x

Inspired by the architectures of MOFs and COFs,[52-55] we demonstrate a simple and fundamental principle that starts with versatile building blocks containing both coordination sites and covalent reactive groups (**Type III, Figure 1**). Thanks to the geometry of coordination behavior, the chelation between metal ions and such linkers leads to multi-dimensional rigid complexes with organic groups at the end serving as secondary building units (SBUs), followed by the polymerization or polycondensation themselves or in the presence of another organic linker.[39, 56-57] Actually, pioneer works for the synthesis of MOF-901 and COF-505 have already been present by Yaghi group with Type III building units such as: 4-aminobenzoic acid or 4,4'-(1,10-phenanthroline-2,9-diyl) dibenzaldehyde.[58-59] Directed by the principle above, coordination-supported organic polymers (COPs)-a class of inorganic-organic hybrids, are reported here and shown with exceptional properties including uniform mesoporous structure, high surface area (up to 1123 m^2g^{-1}), and good stability in water and air (up to 400°C).

The bifunctional 5-amino-8-hydroxyquinoline (AHQ) was selected as the building unit, which can not only form well-known complexes with metal ions through chelation, but also undergo the covalent bonding with organic aldehyde/acid/acid anhydride by the amino group at the eight position. It is well acknowledged that 8-hydroxyquinoline with a bidentate structure is a much stronger donor than the aromatic amino.[60-61] The chelating of $Al(NO_3)_3$ by AHQ with a molar ratio of 1: 3 in N,N-dimethylformaldehyde (DMF) led to an octahedral stable complex (Al-AHQ) **(Scheme 1)**, which was well characterized by NMR, FTIR and elemental analysis.[62] Interestingly, the rigid Al-AHQ with three amino groups at the edge is a potential SBU, which is ready to be connected through imine or imide condensation processes.[63] In this case, we chose tetrakis(4-formylphenyl)-silane (TFS) with four aldehyde groups or abundant pyromellitic dianhydride (PMDA) as linkers. The polycondensation of Al-AHQ and PMDA or TFS were performed in 1-methyl-2-pyrrolidinone (NMP) and DMF at 100-170°C for 48 h. Then, red powder (COP-1) and brown yellow powder (COP-2) were isolated from the solution, followed by washing, soxhlet extracting in ethanol and drying in vacuum. The corresponding yields were 86% and 72% based on AHQ.

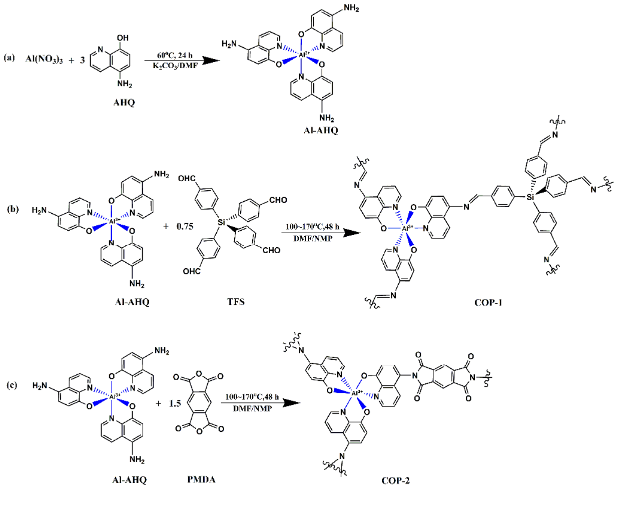

Scheme 1. The synthetic routes to COPs.

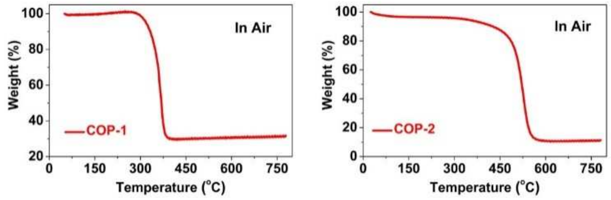

Figure 2. The TGA curves of COPs in air. (Heating rate: 10 °C min^{-1})

The connection of Al-AHQ and TFS was suggested in fourier transform infrared (FTIR) spectroscopy of COP-1, where a characteristic peak at 1615 cm^{-1} relating to the C=N stretching vibration was observed (**Figure S1**). Meanwhile, the connection between Al-AHQ and PMDA was suggested in FTIR spectroscopy of COP-2, where a group of typical peaks for the phthalimide linkage were observed, including the sorption bands at 1781 cm^{-1} and 1714 cm^{-1} due to the asymmetric and symmetric vibrations of the C=O group, and the peak at 1377 cm^{-1} corresponding to the stretching vibration of the C–N–C moiety of five-member imide ring (**Figure S2**). The molecular backbones of COPs were also assessed with solid-state ^{13}C cross-polarization magic angle spinning (CP/MAS) NMR. The attribution of those peaks was justified by ^{13}C NMR studies of Al-Tri(8-hydroxyquinoline) and phthalimide.[64-65] In the case of COP-2, the peak A at 166 ppm was assigned to the imide carbon atom, while the peak B at 160 ppm corresponded to the carbon at the eight position of AHQ, next to phenolic -OH group. The carbon atoms (2-, 4- and 9-positions of AHQ) in the pyridine ring showed a high chemical shift of 144 ppm (Peak C). Peaks D-E were attributed to the aromatic carbons at the β-position of the electron withdrawing groups. The signals at around d=121~112 ppm can be assigned to the normal aromatic carbons (**Figure S3**).

Furthermore, we performed the thermogravimetric analysis (TGA) in air, and both COP materials offered good stability. Especially, COP-2 displayed an exceptional thermal

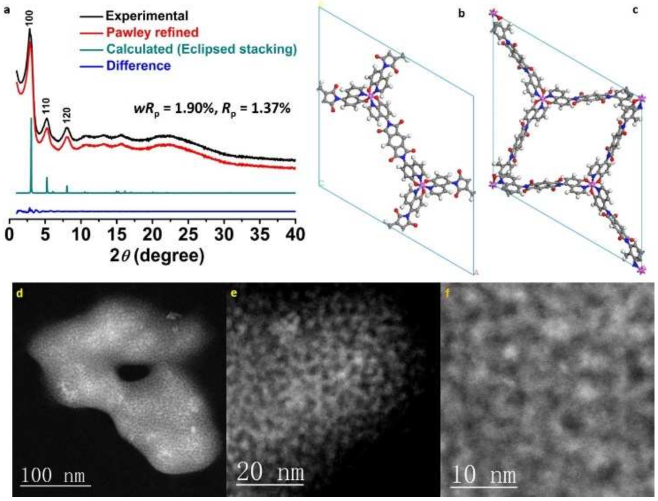

Figure 3. (a) PXRD patterns of COP-2 with the observed profile in black, refined in red, calculated based on the *P*6 topology in teal color, and the difference (observed minus refined) in blue. (b) Structural views of COP-2 in Staggered stacking mode and (c) Eclipsed stacking mode. (d-f) STEM-HAADF images of COP-2.

stability with the decomposition occurring above 400 °C in air, which could be listed as one of the most stable porous coordination polymers **(Figure 2).** The strong Al^{3+}-AHQ chelation together with stable aromatic polyimide linker may contribute to this feature. The crystalline structures of COPs were then investigated by powder X-ray diffraction (PXRD) analysis. The COP-1 afforded no clear peaks, suggesting its amorphous structure (**Figure S4**). Actually, imine condensation reaction is a well-established process for ordered crystalline COFs, because the reversibility of the reaction offers error-correction features. Multiple attempts without acid catalysts, to synthesize crystalline COP-1 failed because the Al-AHQ complex can decompose in acid condition (**Note S1**). Therefore, we reason that the polycondensation between Al-AHQ and TFS may proceed too slowly without any reversibility under acid-free condition, thus resulting in amorphous solid.

Interestingly, the PXRD pattern of COP-2 showed multiple peaks in the 2θ range of 2.80°, 5.25°, 8.06°, 10.71° and 13.15° (**Figure 3a**), which were different to any starting precursors (**Figure S5-S6**), indicating the formation of certain structure orderliness in the sample. To elucidate the lattice packing, a geometrical energy minimization by using the Materials Studio Software package based on the *P*6 topology of eclipsed stacking model was performed, and the unit cell parameters were determined (**Figure 3b, Table S1**).[66] The COP-2 sample exhibited hexagonal unit cells with a=b=33.07°, c=5.58°, $\alpha=\beta=90°$, $\gamma=120°$. The calculated PXRD pattern by the simulated structure agreed with the experimental one. Moreover, the Pawley refinement offered a PXRD pattern, which is in good agreement with the experimental pattern, as suggested by their tiny difference. The final wR_p and R_p values were 1.90% and 1.37%, respectively. It seems like that the unit cell parameters are nearly equivalent to the predictions with excellent agreement factors. Another possible structure based on the *P*63 topology of staggered stacking model resulted in an unmatched PXRD pattern (**Figure 3c, Figure S7, Table S2**).

To inquire the porous morphology of COPs, scanning transmission electron microscopy in high-angle angular dark field mode (STEM-HAADF) was carried out at 60 kV. It is worthy noted that a rapid decomposition of COP-2 occurred if a strong electron beam (e.g., 200 kV) was used. A great quantity of continuous pores staying side by side were observed in a domain of several hundred nanometers (**Figure 3d**). High resolution STEM-HAADF images showed a number of mesopores with the sizes of 2~3 nm and the pore walls with some ordered array roughly followed the crystalline packing of COP-2 (**Figure 3e-3f**).

The porosity of the COP samples was then determined by N_2 adsorption-desorption analysis at 77 K. The N_2 sorption isotherm of COP-1 exhibits a type-IV curve with a distinct capillary condensation step at relative pressure around 0.7~1.0, revealing the presence of large mesopores. The pore size distribution derived from the adsorption branch by using BJH model locates in 8~20 nm. Meanwhile, a BET specific surface area of 646 m^2g^{-1} with a high pore volume of 0.96 cm^3g^{-1} was obtained for COP-1 (**Figure 4a-4b**). The large mesoporous architecture of COP-1 with a high pore volume may be the result of interstitial porosity.

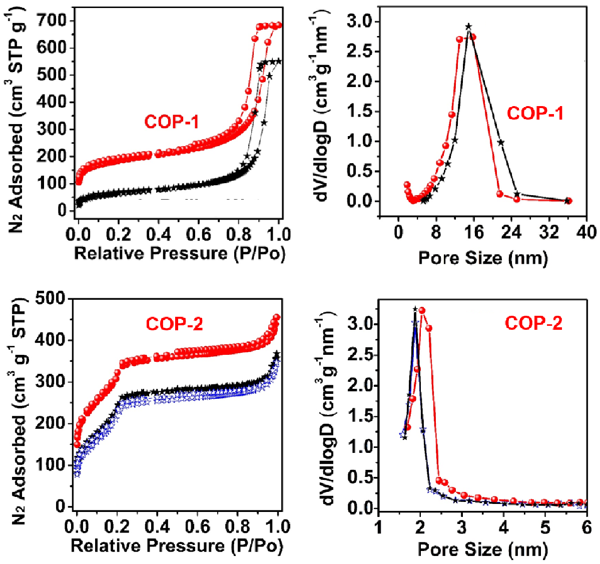

Figure 4. N_2 sorption isotherms (77 K) and the corresponding pore size distributions of COPs (Red ball: COPs, Black solid star: treated in boiling water for 24 h, Blue hollow star: treated in boiling water for 48 h).

Interestingly, COP-2 possessed a sorption isotherm between type I and type IV **(Figure 4c-4d)**. The significant N_2 uptake at $P/P_0<0.05$ indicates the presence of abundant micropores, and at the same time the sharp step observed at $P/P_0=0.05\sim0.25$ suggests condensation sorption in mesopores with a narrow distribution. There is no hysteresis observed in desorption branch, which is actually often observed in mesoporous materials containing hexagonally aligned channels. The COP-2 affords an extremely narrow pore size distribution, centered at 2.5 nm, which agrees well with both structure model and STEM images **(Figure 3b)**. In addition, the BET specific surface area of COP-2 reaches 1123 m^2g^{-1}, a high value for mesoporous material. The CO_2 adsorption isotherms of COP materials at 298 K were then measured, and COPs offered moderate CO_2 adsorption behaviors (**Figure S8**).

To check the water stability of COPs, the samples were immersed in boiling water for 24 h. The recovery yields for COP-1 and COP-2 are 94% and 93%, respectively. The FTIR spectra of COPs before and after the water treatment retained the same sorption peaks, revealing the preserve of characteristic organic groups (**Figures S9~S10**). In addition, the PXRD pattern of COP-2 after being soaked in water remained similar, and the crystalline structure was almost kept (**Figure S11**). Furthermore, the N_2 sorption isotherm of treated COPs maintained a similar profile with the pristine one, except for some decreases in the initial N_2 uptakes, which may be induced by the collapsing of partial micropores (**Figure 4a and 4c**). Clear decreases on surface area were also observed after treated in boiling water (COP-1: 232 m^2g^{-1}, COP-2: 927 m^2g^{-1}). Fortunately, the mesopore size distribution of treated COPs did not change (**Figure 4b and 4d**). Thus, the porous structure with a high surface area can somewhat survive in the harsh treatment of boiling water. [67]

In summary, we have introduced an efficient and simple strategy for the construction of stable coordination-supported porous polymer. By borrowing the ideas from MOFs and COFs, a versatile precursor AHQ was assembled by coupling inorganic chelation and organic polycondensation to build the COPs. The COP-1 has a large mesoporous architecture with a high pore volume, while the COP-2 is rich in mesopores with a high surface area of 1123 m^2g^{-1}, which possesses a well crystalline structure with *P*6 topology. Importantly, the metal-supported backbone of COPs can tolerate water, as a result of the stable chelation and polyimide bonding linkages. Current principle after the careful selection of bifunctional precursors may produce a class of stable coordination-supported porous polymer.

Conflicts of interest

There are no conflicts to declare.

Acknowledges

This paper was prepared in honor of Professor Ruren Xu for his forty-year contribution in zeolitic materials research. SD would like to thank Prof. Xu for his guidance and support over years. P. F. Z. and S. D. were supported by the U.S. Department of Energy, Office of Science, Basic Energy Sciences, Chemical Sciences, Geosciences, and Biosciences Division. The electron microscopy at ORNL (S. Z. Y.) was supported by the U.S. Department of Energy, Office of Science, Basic Energy Sciences, Materials Sciences and Engineering Division. P. F. Z. acknowledges Shanghai Pujiang Program (Grant No. 17PJ1403500), Young Thousand Talented Program and National Natural Science Foundation of China (Grant No. 21776174) for the partial support.

References

1 A. Thomas, F. Goettmann, M. Antonietti, *Chem. Mater.*, 2008, **20**, 738.
2 L. J. McCormick, S. A. Morris, A. M. Slawin, S. J. Teat, R. E. Morris, *CrystEngComm*, 2016, **18**, 1123.
3 J. Tian, P. K. Thallapally, B. P. McGrail, *CrystEngComm*, 2012, **14**, 1909.
4 Z. Xiang, D. Cao, *J. Mater. Chem. A*, 2013, **1**, 2691.
5 J. R. Holst, A. Trewin, A. I. Cooper, *Nat. Chem.*, 2010, **2**, 915.
6 P. K. Thallapally, B. P. Mcgrail, S. J. Dalgarno, H. T. Schaef, J. Tian, J. L. Atwood, *Nat. Mater.*, 2008, **7**, 146.
7 P. Nugent, Y. Belmabkhout, S. D. Burd, A. J. Cairns, R. Luebke, K. Forrest, T. Pham, S. Ma, B. Space, L. Wojtas, M. Eddaoudi, M. J. Zaworotko, *Nature,* 2013, **495**, 80.
8 J. Rabone, Y. F. Yue, S. Y. Chong, K. C. Stylianou, J. Bacsa, D. Bradshaw, G. R. Darling, N. G. Berry, Y. Z. Khimyak, A. Y. Ganin, P. Wiper, J. B. Claridge, M. J. Rosseinsky, *Science* 2010, **329**, 1053.
9 P. Kaur, J. T. Hupp, S. T. Nguyen, *ACS Catal.*, **2011**, *1*, 819.
10 Y. Zhang, S. N. Riduan, *Chem. Soc. Rev.*, 2012, **41**, 2083.
11 J. S. Seo, D. Whang, H. Lee, S. I. Jun, J. Oh, Y. J. Jeon, K. Kim, *Nature*, 2000, **404**, 982.
12 Y. Liu, K. Landskron, *J. Mater. Chem. A*, 2017, **5**, 23523.
13 J. Roeser, D. Prill, M. J. Bojdys, P. Fayon, A. Trewin, A. N. Fitch, M. U. Schmidt, A. Thomas, *Nat. Chem.*, 2017, **9**, 977.
14 T. R. Cook, Y. R. Zheng, P. J. Stang, *Chem. Rev.*, 2013, **113**, 734.
15 H. Furukawa, F. Gandara, Y. B. Zhang, J. Jiang, W. L. Queen, M. R. Hudson, O. M. Yaghi, *J. Am. Chem. Soc.,* 2014, **136**, 4369.
16 R. K. Totten, Y. S. Kim, M. H. Weston, O. K. Farha, J. T. Hupp, S. T. Nguyen, *J. Am. Chem. Soc.*, 2013, **135**, 11720.
17 B. Li, H. M. Wen, Y. Cui, W. Zhou, G. Qian, B. L. Chen, *Adv. Mater.*, 2016, **28**, 8819.
18 M. C. Das, S. Xiang, Z. Zhang, B. L. Chen, *Angew. Chem. Int. Ed.*, 2011, **50**, 10510.
19 A. P. Cõté, A. I. Benin, N. W. Ockwig, M. ÒKeeffe, A. J. Matzger, O. M. Yaghi, *Science*, 2005, **310**, 1166.
20 D. Yuan, W. Lu, D. Zhao, H. C. Zhou, *Adv. Mater.*, 2011, **23**, 3723.
21 T. Ben, H. Ren, S. Ma, D. Cao, J. Lan, X. Jing, W. Wang, J. Xu, F. Deng, J. M. Simmons, S. Qiu, G. Zhu, *Angew. Chem. Int. Ed. Engl.*, 2009, **48**, 9457.
22 P. Kuhn, M. Antonietti, A. Thomas, *Angew. Chem. Int. Ed. Engl.*, 2008, **47**, 3450.
23 N. B. McKeown, P. M. Budd, *Chem. Soc. Rev.*, 2006, **35**, 675.
24 Q. Chen, M. Luo, P. Hammershoj, D. Zhou, Y. Han, B. W. Laursen, C. G. Yan, B. H. Han, *J. Am. Chem. Soc.*, 2012, **134**, 6084.
25 G. H. Bertrand, V. K. Michaelis, T. C. Ong, R. G. Griffin, M. Dinca, *PNAS*, 2013, **110**, 4923.
26 N. C. Burtch, K. S. Walton, *Acc. Chem. Res*., 2015, **48**, 2850.
27 F. P. Doty, C. A. Bauer, A. J. Skulan, P. G. Grant, M. D. Allendorf, *Adv. Mater.*, 2009, **21**, 95.
28 A. Fateeva, P. A. Chater, C. P. Ireland, A. A. Tahir, Y. Z. Khimyak, P. V. Wiper, J. R. Darwent, M. J. Rosseinsky, *Angew. Chem. Int. Ed. Engl.*, 2012, **51**, 7440.
29 P. Horcajada, C. Serre, M. Vallet-Regi, M. Sebban, F. Taulelle, G. Ferey, *Angew. Chem. Int. Ed. Engl.*, 2006, **45**, 5974.
30 Z. Zhang, Q. Yang, X. Cui, L. Yang, Z. Bao, Q. Ren, H. Xing, *Angew. Chem. Int. Ed.*, 2017, **129**, 16500.
31 G. C. Shearer, S. Chavan, S. Bordiga, S. Svelle, U. Olsbye, K. P. Lillerud, *Chem. Mater.*, 2016, **28**, 3749.
32 Q. Chen, J. Sun, P. Li, I. Hod, P. Z. Moghadam, Z. S. Kean, R. Q. Snurr, J. T. Hupp, O. K. Farha, J. F. Stoddart, *J. Am. Chem. Soc.*, 2016, **138**, 14242.
33 W. Li, A. Thirumurugan, P. T. Barton, Z. Lin, S. Henke, H. H. Yeung, M. T. Wharmby, E. G. Bithell, C. J. Howard, A. K. Cheetham, *J. Am. Chem. Soc.*, 2014, **136**, 7801.
34 K. Manna, P. Ji, F. X. Greene, W. Lin, *J. Am. Chem. Soc.*, 2016, **138**, 7488.
35 X. Cui, K. Chen, H. Xing, Q. Yang, R. Krishna, Z. Bao, H. Wu, W. Zhou, X. Dong, Y. Han, B. Li, Q. Ren, M. J. Zaworotko, B. Chen, *Science*, 2016, **353**, 141.
36 J. A. Hurd, R. Vaidhyanathan, V. Thangadurai, C. I. Ratcliffe, I. L. Moudrakovski, G. K. Shimizu, *Nat. Chem.*, 2009, **1**, 705.
37 S. Sakaida, K. Otsubo, O. Sakata, C. Song, A. Fujiwara, M. Takata, H. Kitagawa, *Nat. Chem.*, 2016, **8**, 377.
38 J. E. Bachman, Z. P. Smith, T. Li, T. Xu, J. R. Long, *Nat. Mater.*, 2016, **15**, 845.
39 H. Furukawa, K. E. Cordova, M. ÒKeeffe, O. M. Yaghi, *Science*, 2013, **341**, 1230444.
40 X. Wang, Y. Zhang, H. Zhang, *Angew. Chem. Int. Ed.* 2016, **55**, 4542.
41 N. C. Burtch, H. Jasuja, K. S. Walton, *Chem. Rev.*, 2014, **114**, 10575.
42 P. Deria, D. A. Gomez-Gualdron, W. Bury, H. T. Schaef, T. C. Wang, P. K. Thallapally, A. A. Sarjeant, R. Q. Snurr, J. T. Hupp, O. K. Farha, *J. Am. Chem. Soc.*, 2015, **137**, 13183.
43 P. Zhang, H. Li, G. M. Veith, S. Dai, *Adv. Mater.*, 2015, **27**, 234.

44 W. Lu, D. Yuan, D. Zhao, C. I. Schilling, O. Plietzsch, T. Muller, S. Bräse, J. Guenther, J. Blümel, R. Krishna, Z. Li, H. C. Zhou, *Chem. Mater*. 2010, **22**, 5964.
45 D. Wu, F. Xu, B. Sun, R. Fu, H. He, K. Matyjaszewski, *Chem. Rev*., 2012, **112**, 3959.
46 X. Feng, X. Ding, D. Jiang, *Chem. Soc. Rev.*, 2012, **41**, 6010.
47 J. X. Jiang, F. Su, A. Trewin, C. D. Wood, H. Niu, J. T. A. Jones, Y. Z. Khimyak, A. I. Cooper, *J. Am. Chem. Soc.*, 2008, **130**, 7710.
48 M. G. Schwab, B. Fassbender, H. W. Spiess, A. Thomas, X. Feng, K. Mullen, *J. Am. Chem. Soc.* 2009, **131**, 7216.
49 S. Xu, Y. Luo, B. Tan, *Macromol Rapid Commun.*, 2013, **34**, 471.
50 M. J. Neufeld, B. R. Ware, A. Lutzke, S. R. Khetani, M. M. Reynolds, *ACS Appl. Mater. Interfaces*, 2016, **8**, 19343.
51 B. L. Hou, D. Tian, J. Liu, L. Z. Dong, S. L. Li, D. S. Li, Y. Q. Lan, *Inorg. Chem.*, 2016, **55**, 10580.
52 B. Li, H. M. Wen, Y. Cui, W. Zhou, G. Qian, B. Chen, *Adv. Mater.*, 2016, **28**, 8819.
53 M. C. Das, S. Xiang, Z. Zhang, B. Chen, *Angew. Chem. Int. Ed. Engl.*, 2011, **50**, 10510.
54 Y. Liu, K. Landskron, *J. Mater. Chem. A*, 2017, **5**, 23523-23529.
55 J. Roeser, D. Prill, M. J. Bojdys, P. Fayon, A. Trewin, A. N. Fitch, M. U. Schmidt, A. Thomas, *Nat. Chem.*, 2017, **9**, 977.
56 Y. Liu, J. F. Eubank, A. J. Cairns, J. Eckert, V. C. Kravtsov, R. Luebke, M. Eddaoudi, *Angew. Chem. Int. Ed. Engl.*, 2007, **119**, 3342.
57 K. Wang, D. Feng, T. F. Liu, J. Su, S. Yuan, Y. P. Chen, M. Bosch, X. Zou, H. C. Zhou, *J. Am. Chem. Soc.*, 2014, **136**, 13983.
58 H. L. Nguyen, F. Gandara, H. Furukawa, T. L. Doan, K. E. Cordova, O. M. Yaghi, *J. Am. Chem. Soc.*, 2016, **138**, 4330.
59 Y. Liu, Y. Ma, Y. Zhao, X. Sun, F. Gándara, H. Furukawa, Z. Liu, H. Zhu, C. Zhu, K. Suenaga, P. Oleynikov, A. S. Alshammari, X. Zhang, O. Terasaki, O. M. Yaghi, *Science*, 2016, **351**, 365.
60 K. F. Sugawara, H.H.Weetall, G. D. Schucker, *Anal. Chem.*, 1974, **46**, 489.
61 R. Cherdtrakulkiat, S. Boonpangrak, N. Sinthupoom, S. Prachayasittikul, S. Ruchirawat, V. Prachayasittikul, *Biochem Biophys. Rep.*, 2016, **6**, 135.
62 V. M. Manninen, W. A. E. Omar, J. P. Heiskanen, H. J. Lemmetyinen, O. E. O. Hormi, *J. Mater. Chem.*, 2012, **22**, 22971.
63 P. Zhang, X. Jiang, S. Wan, S. Dai, *J. Mater. Chem. A*, ***2015**, 3*, 6739.
64 R. Katakura, Y. Koide, *Inorg. Chem.*, 2006, **45**, 5730.
65 Q. Zhao, K. Chen, W. Zhang, J. Yao, H. Li, *J. Mol. Catal. A: Chem.*, 2015, **402**, 79.
66 *Materials Studio ver. 7.0*, Accelrys Inc.: San Diego, CA.
67 Q. Fang, Z. Zhuang, S. Gu, R. B. Kaspar, J. Zheng, J. Wang, S. Qiu, Y. Yan, *Nat. Commun.*, 2014, **5**, 4503.